Doubly differential cross sections of secondary electrons ejected from gases by electron impact: 50–300 eV on helium

T. W. Shyn and W. E. Sharp
Space Physics Research Laboratory, Department of Atmospheric and Oceanic Science, The University of Michigan, Ann Arbor, Michigan 48109
(Received 29 June 1978)

Doubly differential cross sections of secondary electrons ejected from He by electron impact have been measured utilizing a crossed-beam method. The incident energies used were 50, 100, 200, and 300 eV. The energy and angular range of the secondary electrons measured were from half of the difference between incident energy and ionization energy to 1.0 eV and from 6° to 156°, respectively, with an emphasis on the measurements of low-energy secondary electrons. The present results have been placed on an absolute scale by using the ionization cross section at 100 eV. The results indicate a strong forward peak for low-energy (< 5 eV) secondaries at angles less than 30°. There is good agreement among the measurements of the high-energy secondary electrons but considerable differences exist in the measurements of the low-energy secondary electrons.

I. INTRODUCTION

Among the interactions of an electron with neutral particles (atoms and molecules), ionization of the particles is one of the physical processes of fundamental importance. Ionization cross sections are important quantities in studies of planetary atmospheres, plasma physics, and radiation physics.

Ionization of He by electron impact has been studied extensively by several authors,[1] primarily to find the total ionization cross section. The absolute doubly differential cross section (DDCS), $d^2\sigma/d\Omega\, dE$ (in angle and energy), of secondary electrons ejected from He by electron impact has been measured by Goodrich[2] with an incident energy of 100 eV within the angular range of 20°–160°. Mohr and Nicoll[3] have measured the relative DDCS with incident energies of 40, 60, 100, and 200 eV and with the angular range of 20°–160°.

Opal *et al.*[4] measured the DDCS for a number of simple gases by a crossed-beam method. Incident energies of 50–2000 eV were used for He, N_2, and O_2, and 500 eV for other gases, with the angular range of 30°–150°. The energy range of secondary electrons measured was 4–200 eV. Oda *et al.*[5] have also measured the DDCS from He and Kr using incident energies of 500 and 1000 eV for the angular range of 10°–130° in a volume experiment (static gas target). The lowest secondary electron energy measured was 24 eV. They found a tendency to a strong forward peak at all secondary energies for He below 15° in their measurements. Very recently, Rudd and DuBois[6] have measured the DDCS of secondary electrons from He with incident energies of 100 and 200 eV over the angular range of 10°–130° by a volume experiment. The lowest energy of secondary electrons measured was 4 eV. Grissom *et al.*[7] have measured the singly differential cross section (SDCS) in energy of secondary electrons for an energy range of 0 to 1 eV for He, Ne, and Ar using a trapped-electron method.

Experimental data on the secondary electrons are available for the energies greater than 4 eV and less than 1 eV, but not between the two energy regions. Also there is a considerable disagreement of DDCS and SDCS among the existing measurements, especially between the result of Opal *et al.* and that of Rudd and DuBois.

Theoretical work on the secondary electrons from He by electron impact has been done by Bell and Kingston[8] in which the Born approximation has been used to calculate the DDCS for the incident energy range of 50–2000 eV. Also substantial progress in the theoretical analysis of experimental data has been made by Kim[9] following the Platzman approach[10] and the Fano approach.[11] This analysis allows a comparison between the energy distribution of secondary electrons (SDCS) from experiment and known photoionization cross sections.

This paper presents the results of an experiment in which the DDCS of secondary electrons ejected from He by electron impact have been measured using a crossed-beam method, with a particular emphasis on low-energy secondary electrons. The incident energies of 50–300 eV have been used. The energy range and angular range of secondary electrons measured were from $\frac{1}{2}(E_i - I)$ [where E_i is the incident energy and I is the ionization potential of He (24.6 eV)], down to 1.0 eV and from 6° to 156°, respectively.

II. APPARATUS AND PROCEDURE

The apparatus shown in Fig. 1 used for the present measurement is basically the same as that used previously for the measurement of electrons elastically scattered from N_2 (Ref. 12) and CO_2 (Ref. 13), and the detailed description can be found in the above references. A brief description of the apparatus is as follows; the apparatus consists of three subsystems, i.e., a rotatable electron monochrometer, a collimated neutral beam source, and a fixed-electron detector on the vacuum chamber wall. The rotatable electron monochrometer produces an electron beam of 10^{-7} A with an energy half-width of 0.2 eV. The angular divergence of the electron beam has been measured to be $\pm 2°$ at an incident energy of 50 eV. It becomes smaller at higher energies. It is also noted that this energy monochrometer has a focusing capability on the electron beam by utilizing an electron lens system. Horizontal and vertical motions of the electron beam are accomplished by a set of deflecting electrodes.

A neutral beam is collimated by a fused capillary array (made of stainless steel 304, 40 μ in diameter, 2 mm long, 50% open area). The collimated neutral beam has an angular width of approximately $\pm 5°$, as shown in Ref. 12.

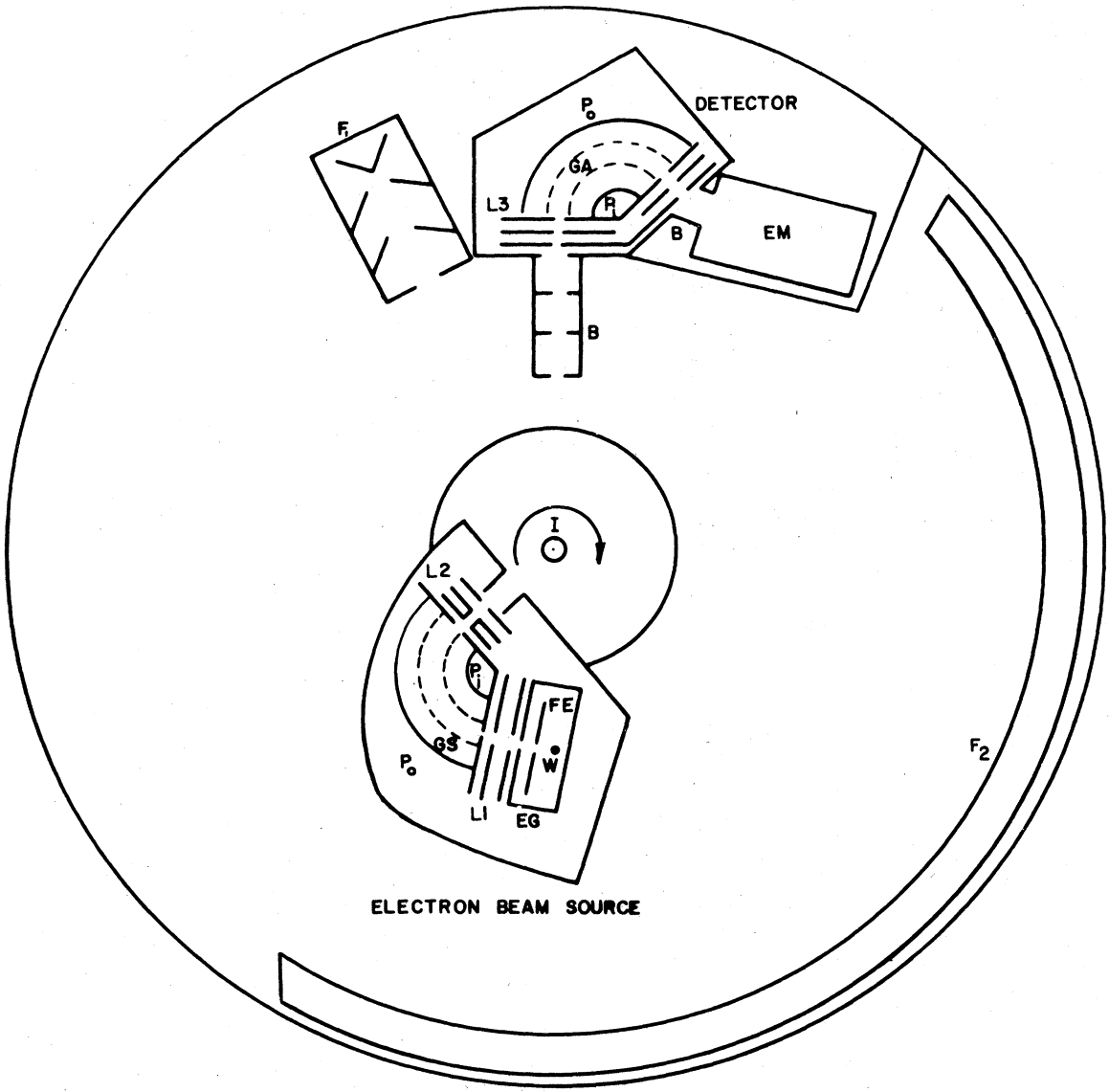

FIG. 1. Schematic diagram of apparatus: W, filament; P_i, inner plate; EG, electron gun; I, interaction region; FE, focus electrode; B, baffle; L1, lens 1; L2, lens 2; L3, lens 3; L4, lens 4; P_0, outer plate; EM, electron multiplier; GS, grids of selector; GA, grid of analyzer; F1 and F2, Faraday cups.

The electron detector system consists of a baffle, an energy analyzer, and an electron multiplier. The acceptance angle of the detector system is ±4°. The energy analyzer is a 127° electrostatic cylindrical type, as shown in Fig. 1. This energy analyzer has two electron collection plates behind the grids in order to collect unnecessary electrons in the detector system. Among the stray electrons, the surface secondary electrons produced off the metal surfaces inside the detector, mainly by the energetic incident electrons, are potentially the most troublesome in the interpreting of the measurements. The production of these surface secondaries in the detector has been measured using an incident electron beam of 100 eV directly into the detector. The intensity of surface secondaries produced in the detector is found to be less than 10^{-5} of the incident beam intensity. The intensity per unit solid angle per unit energy of secondaries from the gases is generally in the order of 10^{-2} of the intensity of the elastically scattered beam per unit solid angle, and, therefore, it is estimated that the surface secondaries contribute one part in 1000 to the signal. Another Faraday cup (F_2 in Fig. 1) has been installed in the system since the two previous measurements. This collects the stray electrons in the system and, at the same time, monitors the strength of the incident electron beam.

The rotatable electron beam interacts at 90° with the collimated neutral beam. Electrons ejected from the neutral beam are detected by the detector system. It is noted that the half-width of the electron beam is inside of the half-width of the collimated neutral beam, and the half-width of the neutral beam is inside of the field of view of the detector system as shown in Ref. 12. The resultant angular resolution of the present experiment is estimated to be ±4° which is sufficient for the secondary-electron measurement by electron impact.

The vacuum enclosure is pumped by a turbomolecular pump (pumping speed of 1500l/sec) down to a pressure of 10^{-8} torr without baking the system. With neutral beam in, the background pressure rises to 2×10^{-4} Torr, and the density of the beam in the interaction region is estimated to be greater than the background density by a factor of 3. At the background pressure of 2×10^{-4} torr the attenuation of ejected electrons from the interaction region to the detector, mainly due to the elastic scattering, has been calculated to be a maximum of 4% at 1 eV and smaller at higher energies. The effect of the high-pressure background to the DDCS measurements is expected to be small (less than 4%), and will be included as a systematic uncertainty in the error analysis.

The magnetic fields in the plane of measurement have been reduced by the three sets of Helmholtz coils and have been measured to be less than 20 mG in all directions. The measurement region is carefully shielded from all exposed potentials.

The absolute energy scale was determined frequently to within 0.05 eV using the He resonance at 19.3 eV.

The detection of the secondary electrons was accomplished by the detector system without the use of any electron lens system in order to insure a constant transmission of the analyzer against energy. The transmission of the analyzer has been measured to be constant within 5% down to an electron energy of 2.0 eV.

The procedure used for the present measurements is as follows: the collimated beam of He is turned on and the signal count is integrated for 10 sec for each electron-beam angle from 12° to 156° in 12° increments for selected incident and secondary-electron energy. In addition, a measurement is also made at 6°. The measurements are repeated with the gas beam off to obtain the background count. The difference between the two signals is the DDCS of secondary electrons ejected from the He beam.

The correction of the final data for volume scattering effects in this experiment is the same as for the elastic scattering, which is measured (because the interaction volume is the same for both cases). First, a system pressure equal to that of the interaction region with the He beam on is established by displacing the capillary from the interaction region. Then the angular dependence of the volume-scattered component of the beam is measured. At 90° (the minimum contribution) this component is (38 ± 1)% of the signal found when the capillary tube is in the interaction region. An uncertainty due to the (38 ± 1)% in the volume correction is ±2%.

III. EXPERIMENTAL RESULTS

The DDCS have been measured at four incident energies, 50, 100, 200, and 300 eV. The energy range of the secondary electrons is from 1.0 eV to $\frac{1}{2}(E_i - I)$, with an emphasis on the low-energy side (<10 eV) and the angular range from 6° to 156°.

Six sets of data for the low-energy secondary electrons and four sets for the rest have been taken and averaged to produce final results for each incident energy. The results have been calibrated among themselves and have been placed on an absolute scale using the total ionization cross sec-

tion of He at 100 eV incident energy measured by Smith.[1] The results are tabulated in Table I, II, III, and IV for the four incident energies, respectively.

The statistical uncertainty in data points for secondary energies less than 3 eV is ± 8% and that for other energies is less than ± 8%. A 10% uncertainty in the calibration among the secondary-electron energies for an incident energy and a 10% uncertainty in the interenergy calibration are contained in the final results. There is an estimated ± 5% uncertainty in the transmission of the electrons through the detector system. An estimated 2% uncertainty in the attenuation factor are used for the experiment. The resultant uncertainty (rms) for the results is thus ± 17%.

Figure 2 shows the DDCS at several secondary energies for a 50-eV incident energy along with the results of Opal *et al.* and the theoretical results of Bell and Kingston. The present results disagree with those of Opal *et al.*, both in value and shape. The results of Opal *et al.* are smaller than the present results by 40% near 90°, and by more than 100% in the extreme angles. Their results at the extreme angles may be due to the overcorrection of the volume effect, as Rudd and DuBois[6] pointed out. The results of the theoretical calculation of Bell and Kingston confirm that the Born approximation is not suitable to apply in this low-energy region.

Figure 3 shows the DDCS at several secondary energies for a 200-eV incident energy beam, along with the experimental results of Opal *et al.* and Rudd and DuBois and the calculation of Bell and Kingston. As shown in Fig. 3, there is a strong forward peak below 15° for all energies (the same is true for 300-eV incident energy, but not for 50 and 100-eV incident energy), as other investigators[5,6] have seen. The DDCS at 200 eV have, in general, flatter angular distributions than those at 50 eV incident. Also there is another peak in the DDCS between 45° and 70° which is due to the conservation of energy and momentum of the colliding system. The peak begins to appear at the secondary-electron energy of 3.0 eV. It moves to higher angles, reaching a maximum angle at 40 eV, then returning to smaller angles as the energy goes higher. The maximum point of the peak approximately follows the conservation laws.

The relative shape of the Opal *et al.* results agrees well with the present results near 90°; however, again there is a disagreement at the extreme angles for all secondary-electron energies. Moreover, the magnitude of the DDCS of Opal *et al.* are larger than the present result by 30% near 90°, and smaller at the extreme angles. The agreement between the present result and that of Rudd and DuBois is good for the backward scattering at all secondary-electron energies. The agreement becomes better as the secondary-electron energy increases, except near an angle of 130°. Comparison with the results of theoretical calculations by Bell and Kingston using the Born approximation show quite good agreement between 60° and 120°, but not at the extreme angles. The calculation does not produce the sharp forward peak below 15°. These facts indicate that the Born approximation is still not as suitable as expected.

Figure 4 shows the SDCS in energy for 50-eV incident energy along with the result of Opal *et al.* and that of Grissom *et al.* Clearly, there is a disagreement among the three results. The result of Grissom *et al.* for 0–1-eV secondary electrons is almost twice as large as the extrapolated value of the present result, while the result of Opal *et al.* is half of the value of the present results. A noteworthy point is that as the energy decreases, the SDCS begins to decrease from about 5 eV. This is contrary to the case of the higher incident energies (see below).

Figure 5 shows the SDCS at 200-eV incident energy along with the results of Opal *et al.*, Rudd and DuBois, and Grissom *et al.* The result of Grissom *et al.* lies in the apparent trend of the present results. The results of Opal *et al.* are larger than the present results by approximately 40% for all secondary energies. However, the general shape of SDCS of Opal *et al.* is in good agreement with the present results except near the energy $\frac{1}{2}(E_i - I)$, where the electron exchange effect comes in. The results of Rudd and Dubois do not agree with the present result very well at high energies.

The results for 100-eV and 300-eV incident energies have almost the same trend as that for 200-eV incident energy.

Table V compares the total ionization cross sections of the present experiment along with the results of Smith,[1] Opal *et al.*,[4] and Rudd and DuBois.[6] As mentioned before, the present results are normalized among the incident energies and secondary-electron energies, and have been placed on an absolute scale using the total ionization cross section of He at 100 eV measured by Smith.[1] Generally the present results agree very well with that of Smith; there is fair agreement within uncertainties among the results of Opal *et al.*, Rudd and DuBois, and the present experiment (the exception being the 50-eV incident energy of Opal *et al.*), even though significant differences in the DDCS exist among the three measurements. The $\sin\Theta$ factor in the calculation of the total cross sections reduces the effect of the DDCS on the total cross sections.

Finally, Fig. 6 shows the Platzman plot for

TABLE I. DDCS ($d^2\sigma/d\Omega dE$) of secondary electrons ejected from He by 50-eV impact energy (in units of 10^{-20}cm^2/ster-eV). (The numbers in parentheses represent extrapolated data points.)

E_s (eV) \ $\theta°$	12	24	36	48	60	72	84	96	108	120	132	144	156	168
1.0	83.6	56.6	36.4	19.4	13.8	13.4	12.3	11.0	11.5	13.8	20.2	23.3	(27.7)	(34.0)
2.0	42.8	29.8	20.1	20.1	15.1	14.5	13.3	13.9	15.8	18.6	23.9	30.4	33.2	(45.0)
3.0	35.1	29.7	17.1	20.3	17.1	17.1	15.2	17.1	18.2	22.7	29.5	37.2	43.3	(55.1)
4.0	36.7	25.9	17.3	19.2	17.4	17.3	15.9	16.6	18.2	23.1	31.2	38.9	45.6	(59.8)
5.0	48.3	28.4	17.4	21.4	18.3	17.1	15.8	17.1	18.9	24.7	32.0	38.7	45.5	(55.7)
6.0	43.5	29.2	19.2	19.2	16.0	14.8	14.5	14.9	16.5	21.3	28.0	35.5	40.7	(49.7)
8.0	41.8	31.8	20.7	18.9	16.5	15.4	15.6	15.8	18.1	22.0	28.1	34.7	41.6	(51.3)
10.0	47.9	35.9	24.2	19.3	15.1	13.4	12.9	13.4	15.2	18.7	24.2	28.8	33.6	(40.7)
12.7	55.7	36.7	20.6	14.0	10.8	9.2	8.4	8.2	9.0	11.1	14.6	18.2	22.1	(27.9)

TABLE II. DDCS ($d^2\sigma/d\Omega\, dE$) of secondary electrons ejected from He by 100-eV impact energy (in units of 10^{-20} cm^2/ster-eV. (The numbers in parentheses represent extrapolated data points.)

E_s (eV) \ $\theta°$	12	24	36	48	60	72	84	96	108	120	132	144	156	168
1.0	170.6	77.2	42.7	30.9	21.7	12.2	10.8	12.2	14.7	18.6	23.1	25.5	(27.4)	(29.4)
2.0	80.3	21.6	18.5	22.4	19.5	19.0	19.3	19.3	21.4	23.5	27.4	31.5	33.9	(36.5)
3.0	57.5	20.8	12.8	20.9	19.6	19.8	17.3	18.7	20.8	22.5	26.6	30.8	37.6	(44.4)
4.0	31.7	16.2	9.5	19.0	18.1	20.0	19.2	18.9	20.4	23.5	25.1	28.5	31.9	(35.5)
5.0	22.0	15.4	11.0	18.0	18.4	19.2	17.9	17.5	17.8	20.6	22.8	26.1	30.6	(35.4)
6.0	23.6	16.7	10.3	15.8	16.5	17.0	16.1	15.8	16.2	18.4	21.6	24.5	26.3	(30.2)
8.0	16.9	11.7	12.3	17.0	16.8	14.6	12.8	12.4	12.4	14.3	17.2	21.7	24.8	(28.1)
10.0	14.1	11.6	13.0	14.6	14.0	13.0	11.7	10.7	10.7	12.0	14.7	17.6	20.2	(22.7)
15.0	13.1	13.1	11.4	11.3	10.3	9.4	8.3	7.6	7.7	8.5	9.2	10.8	12.3	(14.0)
20.0	13.9	10.7	9.1	8.7	7.9	6.6	5.3	4.5	4.3	4.9	5.9	6.6	7.6	(8.8)
25.0	12.6	9.8	7.9	7.1	6.0	4.6	3.6	3.0	3.0	3.3	3.8	4.5	5.1	(6.1)
30.0	15.8	12.1	8.0	5.8	5.0	3.6	2.7	2.3	2.2	2.4	2.8	3.1	3.6	(4.0)
37.7	18.5	13.1	8.0	5.3	3.8	2.7	2.0	1.7	1.5	1.7	1.9	2.2	2.6	(3.0)

TABLE III. DDCS ($d^2\sigma/d\Omega dE$) of secondary electrons ejected from He by 200-eV impact energy (in units of 10^{-20} cm/ster-eV). (The numbers in parentheses represent extrapolated data points.)

E_s (eV) \ $\theta°$	6	12	24	36	48	60	72	84	96	108	120	132	144	156	168
1.0	261.3	140.4	44.2	26.4	15.3	8.9	7.5	7.5	8.5	10.9	14.7	15.1	16.4	(17.8)	(18.8)
2.0	191.5	70.3	44.8	32.1	12.1	10.8	10.3	9.5	10.6	11.7	13.1	13.8	15.9	(17.4)	(20.5)
3.0	121.0	54.3	22.4	18.5	16.1	11.2	10.3	11.6	12.3	12.7	14.0	16.4	17.5	17.6	(18.6)
4.0	131.9	35.2	18.5	11.1	13.3	14.1	13.5	12.7	11.8	12.3	12.8	14.3	15.4	16.5	(17.9)
5.0	75.8	31.9	12.9	8.9	13.7	14.6	13.5	12.5	11.7	11.8	12.9	13.9	15.7	16.6	(17.7)
6.0	57.6	25.0	10.8	8.8	13.1	14.4	13.6	12.7	11.3	11.5	11.9	13.8	14.9	16.3	(18.2)
8.0	29.8	17.9	8.2	7.9	12.3	13.5	12.8	11.2	9.8	9.2	10.2	11.2	12.7	13.8	(15.3)
10.0	22.4	13.6	8.1	9.8	11.4	12.1	10.9	9.5	7.9	7.8	8.0	8.6	10.6	12.1	(13.9)
12.0	18.1	10.0	8.0	8.4	9.8	10.2	9.1	7.6	6.6	5.8	6.3	6.9	8.1	8.9	(10.0)
15.0	19.3	9.3	7.2	7.7	8.7	9.2	8.3	6.5	5.2	4.5	4.8	5.4	6.2	7.3	(8.4)
20.0	16.0	5.3	5.5	6.1	6.8	7.2	6.2	4.7	3.6	3.0	3.1	3.5	4.1	4.8	(5.5)
25.0	11.0	4.8	4.5	5.0	5.8	6.0	4.9	3.6	2.6	2.1	2.2	2.6	2.9	3.4	(3.8)
30.0	11.7	3.4	3.2	3.6	4.4	4.6	3.7	2.6	1.8	1.3	1.4	1.6	1.9	2.1	(2.3)
40.0	6.5	2.2	1.7	2.4	3.0	3.0	2.1	1.3	0.91	0.75	0.75	0.91	1.0	1.1	(1.3)
50.0	5.3	1.7	1.6	1.9	2.1	1.9	1.3	0.79	0.43	0.35	0.39	0.44	0.51	0.57	(0.63)
60.0	3.6	1.5	1.2	1.5	1.7	1.4	0.82	0.48	0.27	0.21	0.26	0.27	0.31	0.36	(0.39)
70.0	3.3	1.9	1.6	1.7	1.6	1.1	0.62	0.32	0.21	0.18	0.18	0.20	0.21	0.25	(0.28)
87.7	4.2	3.5	2.7	2.1	1.4	0.76	0.36	0.22	0.16	0.15	0.12	0.13	0.12	0.15	(0.16)

TABLE IV. DDCS($d^2\sigma/d\Omega\, dE$) of secondary electrons ejected from He by 300-eV impact energy (in units of 10^{-21} cm^2/ster-eV). (The numbers in parentheses represent extrapolated data points.)

E_s (eV) \ $\theta°$	6	12	24	36	48	60	72	84	96	108	120	132	144	156	168
1.0	1244.7	832.8	446.1	201.4	85.1	62.9	59.3	49.1	82.1	106.7	130.1	140.9	150.5	(157.6)	(166.1)
2.0	844.4	431.2	179.7	153.1	121.5	100.0	92.7	104.5	123.2	136.7	137.3	145.9	159.9	(163.9)	(171.8)
3.0	867.8	472.2	216.4	164.6	116.5	108.4	111.1	103.6	108.4	114.9	120.3	117.6	126.8	147.8	(166.2)
4.0	896.9	423.1	172.7	103.1	117.8	118.5	116.7	115.6	109.1	102.1	107.5	109.1	117.8	130.3	(147.7)
5.0	866.4	263.7	126.9	100.5	118.1	117.0	110.9	104.3	103.2	96.1	102.1	112.6	110.9	119.7	(129.6)
6.0	823.3	299.7	170.4	108.9	111.1	118.0	107.9	96.7	88.1	82.2	87.6	92.4	96.7	97.7	(102.1)
8.0	571.2	182.2	84.6	74.3	95.4	104.4	98.8	90.8	81.2	73.8	77.2	86.3	91.4	103.9	(118.1)
10.0	521.0	145.7	86.7	77.8	88.9	93.9	88.4	80.0	66.7	60.6	58.9	66.1	72.2	81.7	(95.6)
12.0	270.0	112.4	79.6	70.6	83.6	86.4	80.2	71.7	58.2	50.8	50.8	54.8	62.7	70.6	(80.8)
15.0	197.0	72.2	56.5	62.7	71.6	72.2	66.6	49.8	42.6	38.6	35.8	39.7	44.2	50.9	(56.5)
20.0	117.8	51.4	48.0	48.0	57.9	57.7	53.0	42.8	31.2	25.4	24.0	26.4	30.9	35.1	(40.0)
25.0	104.2	34.5	34.3	35.0	41.6	45.5	42.0	31.4	22.6	17.2	16.0	18.2	20.1	23.0	(25.5)
30.0	109.1	35.0	32.9	32.1	37.6	39.3	35.2	25.2	17.7	13.4	12.9	13.9	15.7	18.3	(21.3)
40.0	94.0	18.7	13.8	16.7	24.4	25.5	21.9	14.4	8.8	7.0	7.0	7.2	8.3	9.6	(11.1)
50.0	72.6	14.0	11.9	12.3	17.6	19.4	15.5	9.0	4.8	3.3	3.4	3.7	4.4	5.2	(6.3)
65.0	61.9	9.2	7.2	8.7	12.6	13.9	8.8	4.4	2.4	1.7	1.9	1.8	2.3	2.4	(2.7)
80.0	48.9	7.4	6.0	6.9	10.2	9.8	5.5	2.6	1.6	1.0	1.1	1.1	1.3	1.4	(1.6)
100.0	42.3	7.9	6.3	6.4	8.6	6.5	3.0	1.3	0.97	0.86	0.66	0.66	0.66	0.76	(0.86)
120.0	38.7	9.6	7.1	8.0	8.0	4.5	1.8	1.0	0.57	0.53	0.44	0.48	0.57	0.65	(0.72)
137.7	46.2	13.4	9.6	10.3	7.6	3.4	1.7	1.0	0.63	0.63	0.46	0.46	0.49	0.56	(0.67)

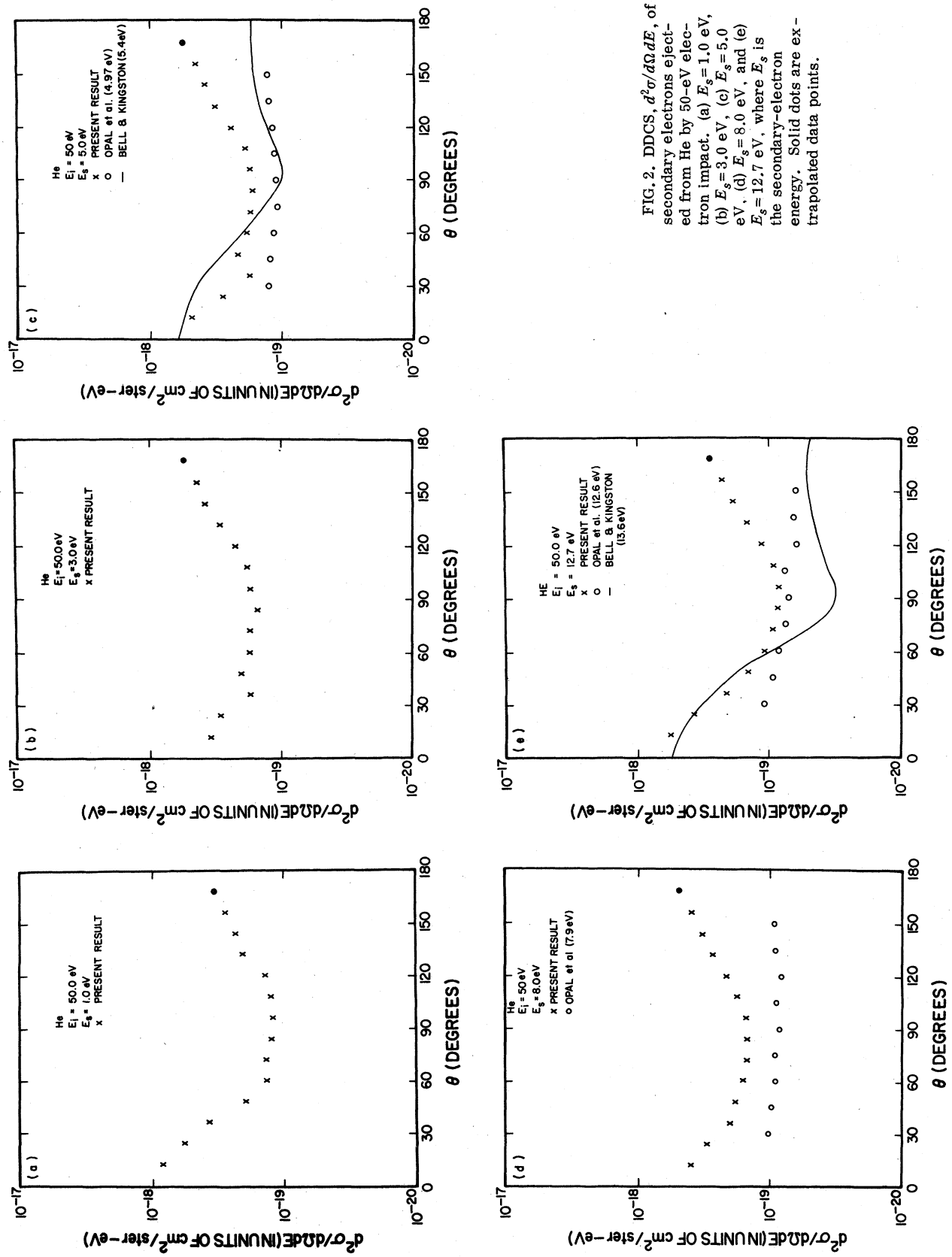

FIG. 2. DDCS, $d^2\sigma/d\Omega\,dE$, of secondary electrons ejected from He by 50-eV electron impact. (a) $E_s = 1.0$ eV, (b) $E_s = 3.0$ eV, (c) $E_s = 5.0$ eV, (d) $E_s = 8.0$ eV, and (e) $E_s = 12.7$ eV, where E_s is the secondary-electron energy. Solid dots are extrapolated data points.

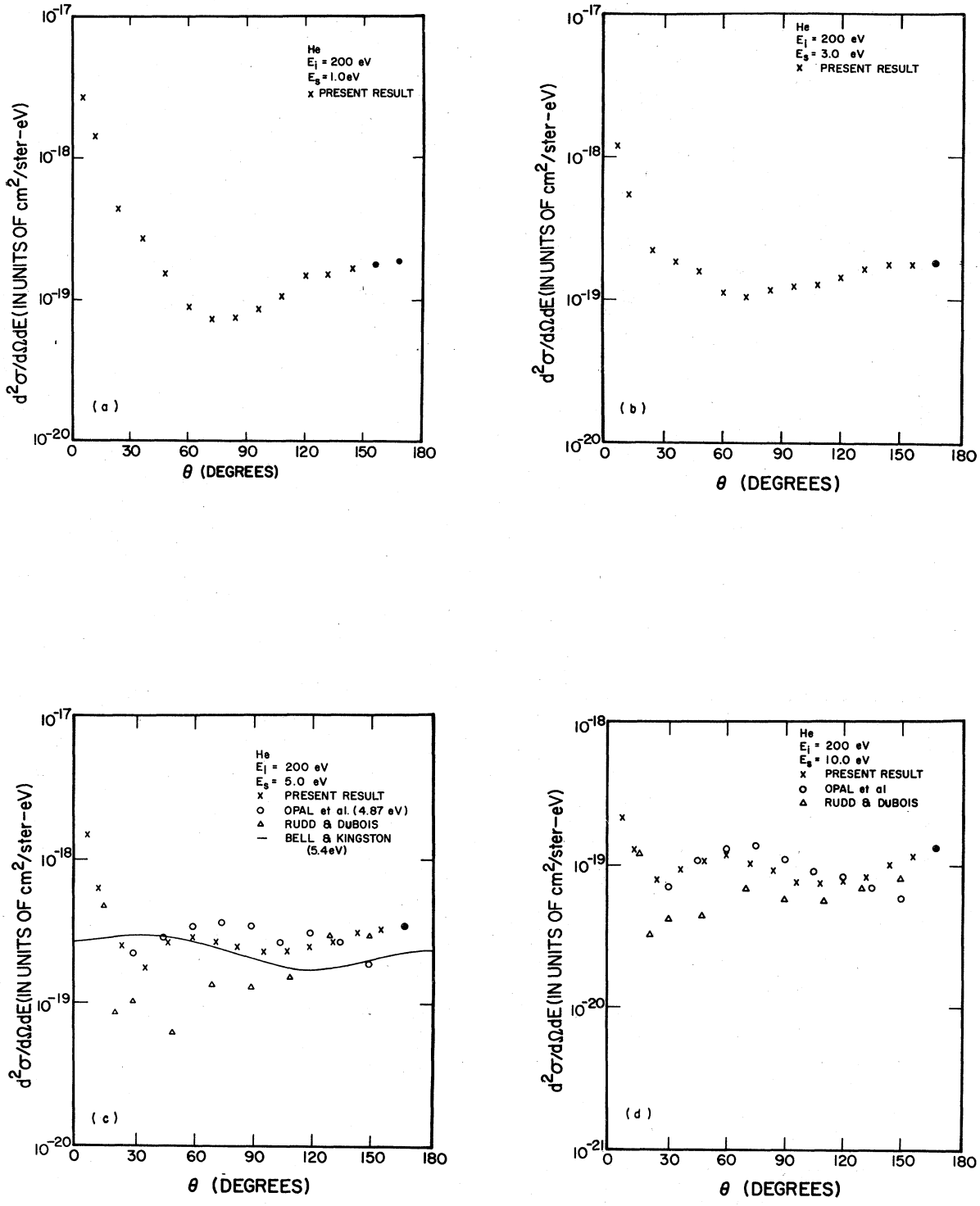

FIG. 3. DDCS, $d^2\sigma/d\Omega\, dE$, of secondary electrons ejected from He by 200-eV electron impact. (a) E_s=1.0 eV, (b) E_s =3.0 eV, (c) E_s=5.0 eV, (d) E_s=10.0 eV, (e) E_s=40 eV, and (f) E_s=87.7 eV, where E_s is secondary-electron energy. Solid dots are extrapolated data points.

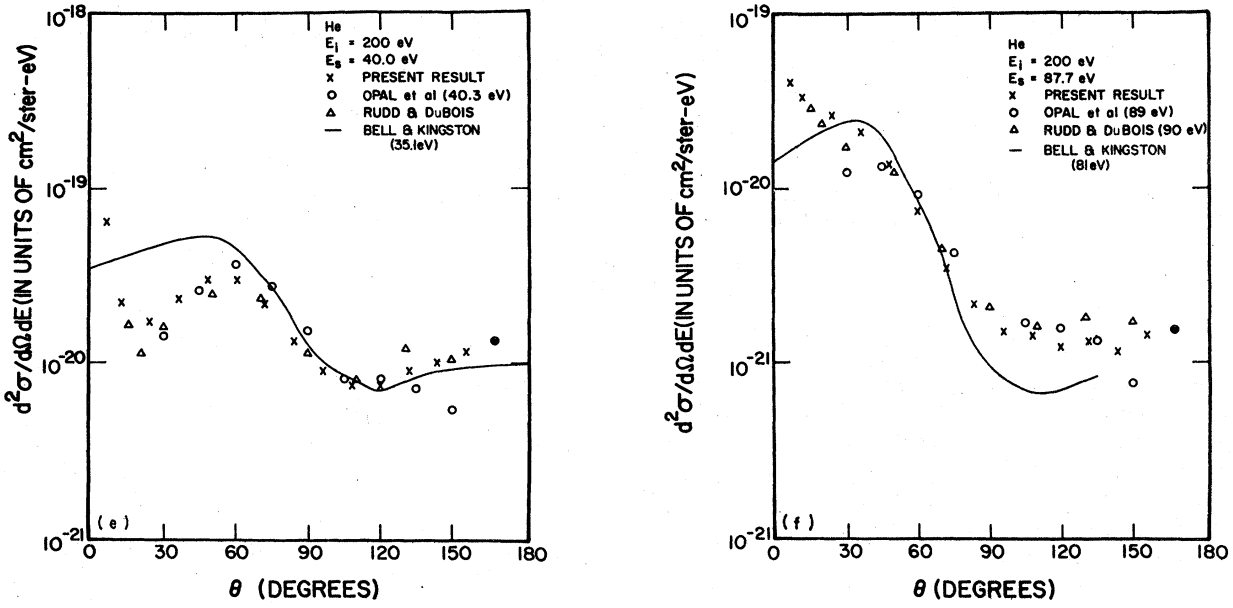

FIG. 3. (*Continued*)

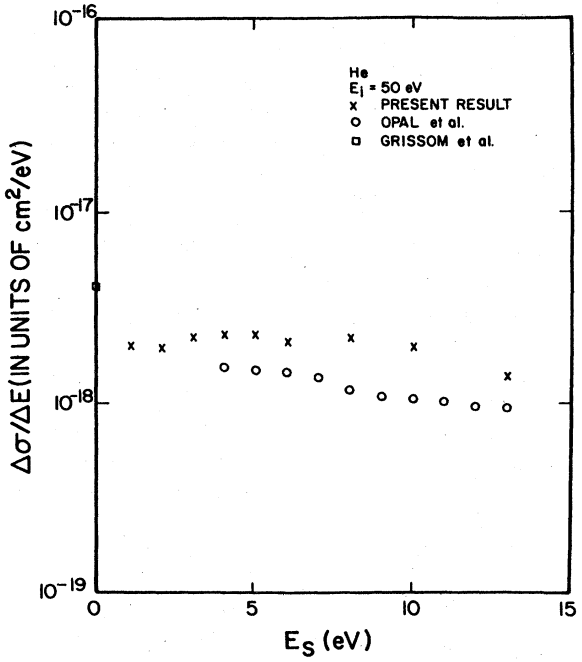

FIG. 4. DDCS, $\Delta\sigma/\Delta E$, of secondary electrons ejected from He by 50-eV electron impact.

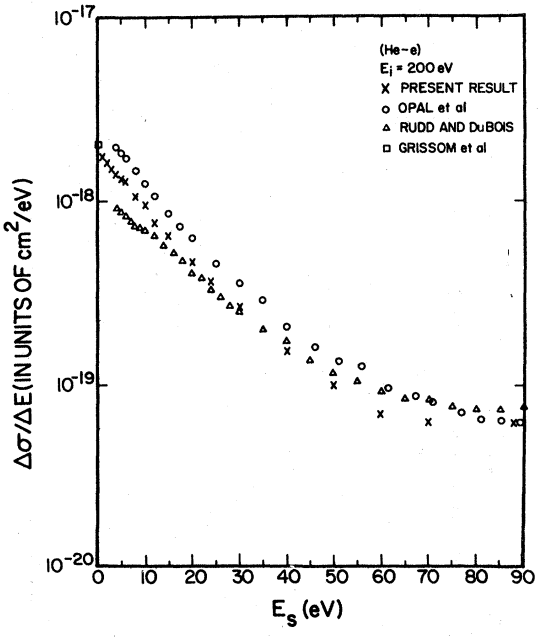

FIG. 5. SDCS, $\Delta\sigma/\Delta E$, of secondary electrons ejected from He by 200-eV electron impact.

TABLE V. Total ionization cross sections of He by electron impact (in units of 10^{-17} cm^2.)

E_i (eV)	Present result	Smith	Opal *et al.*	Rudd and DuBois
50	2.54 ± 0.43	2.44	1.36 ± 0.34	···
100	3.54 ± 0.60	3.54	3.37 ± 0.84	2.96 ± 0.74
200	2.90 ± 0.49	3.22	3.67 ± 0.92	2.34 ± 0.59
300	2.58 ± 0.44	2.74	3.31 ± 0.83	···

four incident energies. The Platzman plot is a graphical scheme whereby the ratio $Y(E)$ of the measured SDCS to the Rutherford cross section per electron is plotted as a function of the inverse of the energy transfer, R/E, of the incident electron to the target particle, where R is the Rydberg energy and E is the energy transfer ($E = E_s + I$). In a Platzman plot $Y(E)$ should approach an effective number of electrons participating in the ionization process for large E, and $Y(E)$ should resemble $E(df/dE)$ in shape for small E, where df/dE is the density of the dipole oscillator strength for ionization. A detailed discussion of the plot can be found elsewhere.[9]

Agreement between the present results and Kim's analysis is generally better as the incident energy increases, since the analysis is based on the Born approximation. The poor agreement at very low secondary-electron energies and near the $\frac{1}{2}(E_i - I)$ energy region may be due in part to inadequacies in the theory.

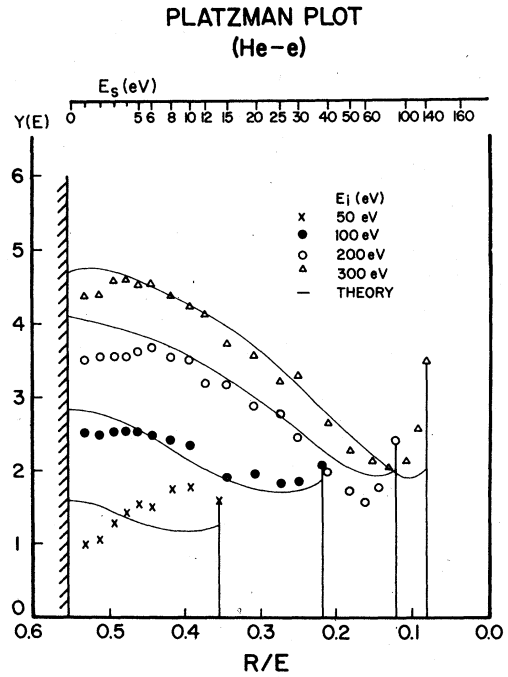

FIG. 6. Platzman plot of secondary electrons ejected from He by 50-, 100-, 200-, and 300-eV electron impact along with the theoretical results by Kim (Ref. 9).

IV. SUMMARY

This paper presents the results of doubly differential cross-section measurements of secondary electrons ejected from He by electron impact utilizing a crossed-beam method. The incident energies, 50, 100, 200, and 300 eV, have been used and the energy and angular range of the secondary electrons measured are from one half of the difference between the incident energy and ionization potential to 1.0 eV and from 6° to 156°, respectively, with a particular emphasis on the low-energy secondary electrons. The uncertainty of the present results is ± 17%.

The present results show that there exists a forward peak in the DDCS of low-energy secondary electrons (< 5 eV) below 30° for the incident energies 50 and 100 eV and a forward peak below 15° in all DDCS of secondary-electron energies for 200- and 300-eV incident energies as many authors[5,6] have observed. The forward peak becomes stronger, in general, as the incident energy increases.

There is a good agreement among the existing measurements for secondary electrons of high energies (> 20 eV) for all incident energies except 50 eV incident, but not so good agreement for low secondary energies (< 20 eV). For the measurements with 50-eV incident energy, the present results do not agree with that of Opal *et al.* in shape, as well as in magnitude.

As expected, the theoretical calculation based on the Born approximation does not agree with the present results, especially for extreme angles.

Finally, the present results shown in the Plotzman plot agree, in general, with the theoretical results of Kim except for the case of 50-eV incident energy. Also, there are some disagreements at low energies and near the highest secondary-electron energies, where the electron exchange effect comes in strongly.

ACKNOWLEDGMENTS

This work is supported by the NSF, Atmospheric Research Section, NSF Grant No. ATM77-27215. The authors are grateful to Dr. Y.-K. Kim at Argonne National Laboratory for many valuable discussions at the various stages of this work.

[1]P. T. Smith, Phys. Rev. 36, 1293 (1930); D. Rapp and P. Englander-Golden, J. Chem. Phys. 43, 1464 (1965); L. J. Kieffer and G. H. Dunn, Rev. Mod. Phys. 38, 1 (1966).
[2]M. Goodrich, Phys. Rev. 52, 259 (1937).
[3]C. B. O. Mohr and T. H. Nicoll, Proc. R. Soc. A 144, 596 (1934).
[4]C. B. Opal, E. C. Beaty, and W. K. Peterson, At. Data 4, 209 (1972).
[5]N. Oda, F. Nishimura and S. Tahira, J. Phys. Soc. Jpn. 33, 462 (1972).
[6]M. E. Rudd and R. D. DuBois, Phys. Rev. A 16, 26 (1977).
[7]J. T. Grissom, R. N. Compton, and W. R. Garrett, Phys. Rev. A 6, 977 (1972).
[8]K. L. Bell and A. E. Kingston, J. Phys. B 8, 2666 (1975).
[9]Y. K. Kim, Radiat. Res. 61, 21 (1975); 64, 96 (1975); 64, 205 (1975).
[10]R. L. Platzman, Int. J. Appl. Radiat. Isot. 10, 116 (1961).
[11]U. Fano, Phys. Rev. 95, 1198 (1954).
[12]T. W. Shyn, R. S. Stolarski, and G. R. Carignan, Phys. Rev. A 6, 1002 (1972).
[13]T. W. Shyn, W. E. Sharp, and G. R. Carignan, Phys. Rev. A 17, 1855, (1978).